Proceedings of the XI DINAME, 28th February - 4th March, 2005 – Ouro Preto – MG – Brazil
Edited by D.A. Rade and V. Steffen Jr. 

# NONLINEAR DYNAMIC BEHAVIOR OF A FLEXIBLE STRUCTURE TO COMBINED EXTERNAL ACOUSTIC AND PARAMETRIC EXCITATIONS

**Demian G. da Silva**
Department of Mechanical Engineering, School of Engineering of Sao Carlos, University of São Paulo,
Av. Trabalhador São-Carlense, 400, São Carlos-SP, 13566-590, Brazil
demian@sc.usp.br

**Paulo S. Varoto**
Department of Mechanical Engineering, School of Engineering of Sao Carlos, University of São Paulo,
Av. Trabalhador São-Carlense, 400, São Carlos-SP, 13566-590, Brazil
varoto@sc.usp.br

***Abstract:*** *Flexible structures are frequently subjected to multiple inputs when in the field environment and in order to accurately determine their dynamic response it is highly desirable to obtain as much information as possible from the excitation sources that act on the system under study. Detailed information include, but are not restricted to appropriate characterization of the excitation sources in terms of their variation in time and in space for the case of distributed loads. Another important aspect related to the excitation sources is how the different inputs contribute to the measured dynamic response. A particular and important driving mechanism that can occur in practical situations is the parametric resonance. Another important input that occurs frequently in practice is related to acoustic pressure distributions that represent a distributed type of loading. In this paper detailed theoretical and experimental investigations on the dynamic response of a flexible cantilever beam carrying a tip mass to simultaneously applied external acoustic and parametric periodic excitations have been performed. A mathematical model for transverse nonlinear vibration is obtained by employing Lagrange's equations where important nonlinear effects such as the beam's curvature and quadratic viscous damping are accounted for in the equation of motion. The beam is driven by two excitation sources, a sinusoidal motion applied to the beam's fixed end and parallel to its longitudinal axis and a distributed sinusoidal acoustic load applied orthogonally to the beam's longitudinal axis. The major goal here is to investigate theoretically as well as experimentally the dynamic behavior of the beam-lumped mass system under the action of these two excitation sources. Results from an extensive experimental work show how these two excitation sources interacts for various testing conditions. These experimental results are validated through numerically simulated results obtained from the solution of the system's nonlinear equation of motion.*
***Keywords:*** *nonlinear vibration, parametric excitation, acoustic excitation, modal interaction.*

## 1 Introduction

In the field environment, a given structure may be subjected to excitations of different nature. This is typically the case of flight hardware, a satellite for example. During the flight, the satellite is subjected to contact excitations arising from the connections with the launch vehicle and possibly acoustic excitations due to internal noise generation mechanisms. A CD player mounted on the dash board of an automobile is another good example of a system that may suffer from multiple excitations. In both cases, the structure needs to survive to all forms of excitations and still operate accordingly, and obviously, this is a major concern of design and test personnel involved with each particular product. In practice, all structures are essentially nonlinear, and in this case the mathematical models used to describe the dynamics of the system are considerably more complex than the models used in the classical linear theory. The type of the nonlinearity present, arising for example from geometry or material property will reflect on differences exhibited by the equations of motion used to model the system´s dynamic behavior. Particularly, one of these differences occurs in the presence of time varying coefficients on the left hand side of the equation of motion, frequently in the term that describes the elastic forces. This term constitutes the parametric excitation (Nayfeh and Mook, 1979 and Cartmell, 1990) and due to this excitation mechanism, the structure may present a special and very important vibration condition, characterized by large amplitudes and that is called parametric resonance.

Zavodney and Nayfeh (1989) performed an extensive theoretical and experimental work in three different slender cantilever beams carrying a lumped mass, two steel and one composite graphite-epoxy beam. In all situations the beams were vertically supported and subjected to a principal parametric base excitation. The slender beam Euler-Bernoulli has been used to derive the governing non-linear partial differential equation and the Galerkin's method was used to obtain the discrete equation of motion. The method of multiple scales was employed to determine an approximate solution for the time domain equation of motion and experiments were carried out on the metallic beams and later on the composite beam. All of the metallic beams has failed prematurely due to the very large response amplitudes caused by the parametric resonance phenomenon.

Cartmell (1990), showed an important work on the derivation of the equation of motion applied to a cantilever beam subjected to base excitation. A similar configuration to that used by Zavodney and Nayfeh (1989) was employed except that in this case, the direction of the excitation was in the transverse direction instead of vertical. Initially, the kinematics of the problem was established and subsequently the Lagrange's formulation was applied to find the equation of motion. The main goal in Cartmell´s work was to illustrate the use of classical engineering theories in the accurate modelling of a

very simple structure, and to highlight the conceptualization of a three-dimensional problem.

Anderson et al. (1996) have performed an experimental and theoretical investigation into the first and second mode responses of a parametrically excited slender cantilever beam without added mass. It has been shown that the inclusion of a quadratic damping in the analytical model significantly improves the agreement between the experimental and theoretical results. In addition, the experimental results obtained verified that the often ignored non-linear curvature terms play a crucial role in the response of the first mode and that the non-linear inertia terms also plays an important role in the response of the second mode.

HaQuang et al. (1987a) performed an important analytical investigation on a weakly quadratic and cubic nonlinear multiple degrees of freedom system including both external and parametric excitations. They used the multiple scales method to investigate the steady state responses when the frequency of the parametric excitation is near a natural frequency of the system for three conditions: (i) no external excitation present; (ii) external excitation present but not involved in the resonance condition; and (iii) external excitation frequency equals the parametric excitation frequency. They used frequency-response curves to illustrate the effects of damping, excitation amplitudes, and a phase difference between the parametric and external excitations. They affirmed yet that the most surprising result was the existence of stable, multi-modal, steady state responses. The same authors (HaQuang, 1987b) published another important and extensive theoretical study focused on the interaction between parametric and external excitations acting on a weakly quadratic and cubic nonlinear system. Essentially the same theoretical approach used in the previous work was employed here to analyze the system's dynamic response to the combined excitations. The authors pointed here to the difficulty in defining suitable control strategies when the combined excitations act on the test structure.

Among the external excitation mechanisms that could act on the structure in the field, acoustic loadings play an important role in several practical situations as for example in the study of fatigue on aircraft surfaces due to acoustic pressure waves generated by the engines (Callinan, 1997). From the laboratory viewpoint, the problem of performing tests in a flexible structure under the combined effect of a parametric and external acoustic excitation is indeed a challenging problem. Based on this argument, the major goal of this paper is to perform a detailed theoretical and experimental investigation on the dynamic response properties of a slender beam-lumped mass system undergoing combined and simultaneous parametric and external acoustic excitations. A nonlinear mathematical model is derived based on energy quantities. Some fundamental preliminary tests are performed in order to obtain the modal properties of the structure and the characterization of the excitation sources. In the sequence, an extensive nonlinear experimental analysis is performed in various testing conditions by simultaneously applying the structural and acoustic excitations to the structure. The system's response is measured and compared with numerically obtained results from the system's model.

## 2 Theoretical Approach

To investigate the effects of the combined excitations from the analytical viewpoint, the structure shown in Figure 1 was built. It is composed of a slender stainless steel ASTM A240 beam, with dimensions of 100 mm in length, 20 mm in width and 1 mm in thickness. The lumped mass is composed of carbon steel ASTM A36, with dimensions of 10 mm in length, 40 mm in width and 20 mm in height. The opposite beam's end is clamped to a rigid base built from carbon ASTM A36 steel.

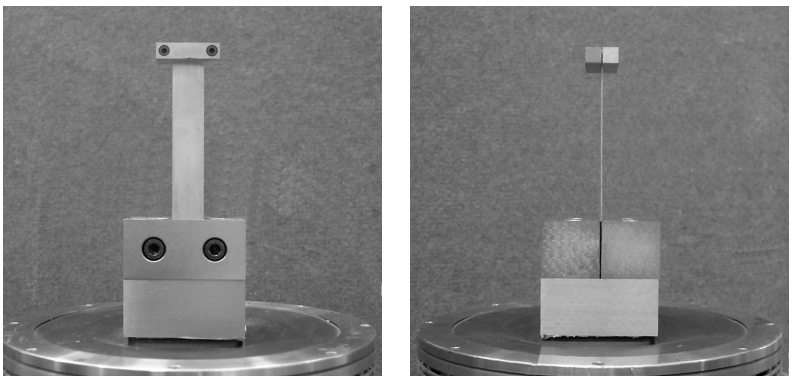

**(a)** **(b)**

Figure 1: Physical system under investigation: (a) frontal view; (b) lateral view.

This structure will be simultaneously submitted to two external driving mechanisms, a parametric excitation due to a base excitation applied by an electrodynamic shaker and a transverse acoustic external excitation applied by an acoustic source positioned parallel to the structure. The following assumptions are made in deriving the equation for the beam's transverse motion:

**H1** The beam's transverse vibration is purely planar and completely described in the $OZX$ plane since the lumped mass is symmetric with respect to the centerline and the beam is kept short (less than thirty times the beam's width) then the torsional modes can be neglected in the analysis.

**H2** The thickness of the beam is small compared to the length so that the effects of shear strain and rotatory inertia of the beam can be neglected.

**H3** All the transverse sections to the centerline of the beam remains plane and normal to the centerline.

**H4** It is assumed that the beam's material obeys the constitutive Hook's law, is isotropic and there is neither plastic strain or internal heat generated during the vibration.

**H5** The mass of the beam when compared with the lumped mass is very small, then its effect can be neglected and the system will contain a single degree of freedom.

**H6** Potential fluid-structure interactions between the acoustic media and the structure under study are neglected, particularly in terms of additional damping added to the system due to the fluid motion caused by the acoustic excitation source.

The physical model shown in Figure 2 was considered. In this model, the $OXYZ$ orthogonal coordinates system is fixed at the base of the beam in its unstressed position and, directed such as the $X$ axis is taken as the centreline of the beam. The origin $O$ of the coordinated system may be subject to a dynamic displacement, but only in the $X$ direction, described by $U_B(t)$. In addition, a distributed acoustic pressure is acting transversely in the $Z$ direction. A generalized coordinated $w(x,t)$ is used to measure the deformation from the unstressed position of an arbitrary axial position $x$ in the $Z$ direction.

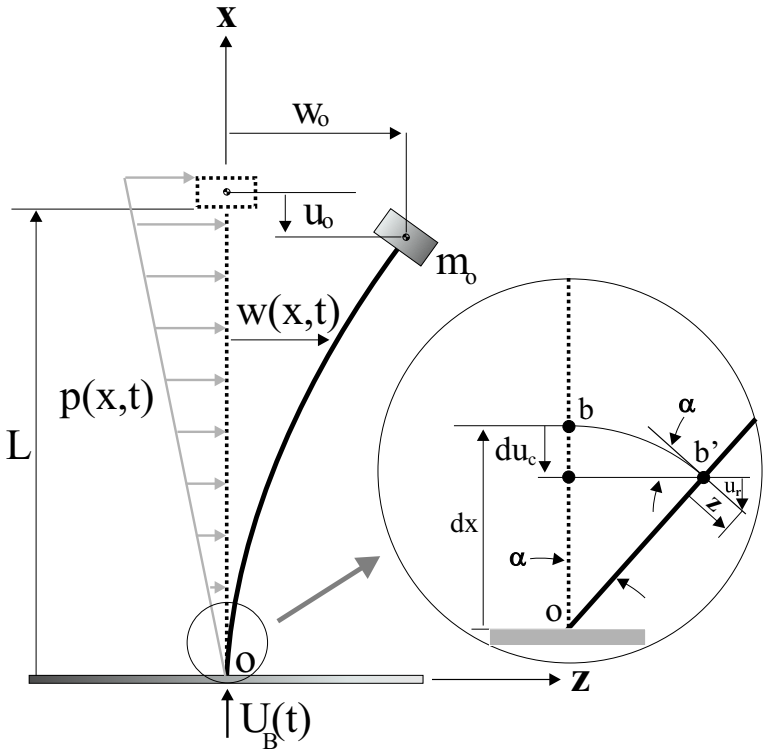


Figure 2: Physical model of the structure under investigation, combined acoustic and base excitations.

When the structure is subject to transverse vibrations with finite amplitude, an imaginary transverse plane normal to the centerline of the beam at point $b$ translates in the $Z$ direction by an amount of $w(x,t)$, also translates in the $X$ direction by an amount of $u_c$, and rotates in the $xz$ plane an amount given by the slope $\partial w/\partial x$ of the deflection curve at point $b$.

From Figure 2 the tangent at the point $P'$ is given by $\tan\alpha = \partial w/\partial x$. Then the angle $\alpha$ at the same point can be written in a series form as

$$\alpha = \frac{\partial w}{\partial x} - \frac{1}{3}\left(\frac{\partial w}{\partial x}\right)^3 + \frac{1}{5}\left(\frac{\partial w}{\partial x}\right)^5 + \dots \tag{1}$$

In addition, the infinitesimal axial contraction $du_c$ measured from the point $b$ at coordinate $(x,z) = (dx,0)$ to the projection of the point $b'$ into the $X$ axis is given as

$$du_c = dx(1-\cos\alpha) = dx\left(1 - 1 + \frac{1}{2}\alpha^2 - \frac{1}{24}\alpha^4 + \dots\right) \tag{2}$$

From the modelling viewpoint it is interesting to express the axial contraction $du_c$ as a function of the lateral displacement $w(x,t)$. Then substitution of Equation (1) into Equation (2) results in

$$du_c = \frac{1}{2}dx\left(\frac{\partial w}{\partial x}\right)^2 - \frac{1}{3}dx\left(\frac{\partial w}{\partial x}\right)^4 + \frac{1}{18}dx\left(\frac{\partial w}{\partial x}\right)^6 + \dots \tag{3}$$

As mentioned earlier the rotation of any transverse section of the beam will produce an additional displacement in the $X$ direction. Accordingly, in considering the bending displacement in the $X$ direction of a point in a cross section of the beam at position $z$ below the centroidal axis in the undeformed geometry results in

$$u_r = -z\sin\alpha = -z\alpha + \frac{1}{6}z\alpha^3 - \frac{1}{120}z\alpha^5 + \dots \tag{4}$$

or by employing Equation (1), $u_r$ can be written as function of the lateral displacement $w(x,t)$ as

$$u_r = -z\frac{\partial w}{\partial x} + \frac{1}{2}z\left(\frac{\partial w}{\partial x}\right)^3 - \frac{7}{40}z\left(\frac{\partial w}{\partial x}\right)^5 + \dots \tag{5}$$

### 2.1 Kinetic and Strain Energies and Nonconservative Generalized Forces

Considering the beam as a continuum solid with displacement field described by $u_i\,(i=1,2,3)$ and $u_i^o\,(i=1,2,3)$ the displacement when $x=L$, the complete kinetic energy of the lumped-mass system can be described by

$$T = \frac{1}{2}\int_V \rho\dot{u}_i\dot{u}_i dV + \frac{1}{2}m_o\dot{u}_i^o\dot{u}_i^o \tag{6}$$

in which the dot denotes time derivative, $\rho$ and $V$ are respectively the material density and volume of the beam, and $m_o$ is the value of the lumped mass. In order to simplify Equation (6), the contribution of the distributed mass of the beam will be ignored as well as the rotatory energy of the lumped mass. Hence, the kinetic energy is simplified to

$$T = \frac{1}{2}m_o\left[(\dot{u}_1^o)^2 + (\dot{u}_3^o)^2\right] \tag{7}$$

The task to find $T$ consists in performing several steps. First, the time derivative of the displacement field must be computed which results in expressions for $(\dot{u}_1)^2$ and $(\dot{u}_3)^2$ . Second, the terms in the right hand side of the expressions of $(\dot{u}_1)^2$ and $(\dot{u}_3)^2$ are described as functions of the $w(x,t)$ and its spatial derivatives. Third, a spatial reduction is necessary so that the deflection on the center of the lumped mass can be obtained. This can be done by using an expression of the form

$$w(x,t) = \phi(x)\,w_o(t) \tag{8}$$

in which $\phi(x)$ represents the first linear natural mode of the structure and $w_o(t)$ represents the modal coordinate associated with this natural mode. As a final result, the expressions for $(\dot{u}_1^o)^2$ and $\left(\dot{u}_3^o\right)^2$ are found and truncated to result in nonlinearities of third order

$$(\dot{u}_1^o)^2 = (A_1)^2 w_o^2\dot{w}_o^2 - 2A_1 w_o\dot{w}_o\dot{U}_B + \frac{8}{3}A_2 w_o^3\dot{w}_o\dot{U}_B + \left(\dot{U}_B\right)^2 \tag{9}$$

$$(\dot{u}_3^o)^2 = \dot{w}_o^2 \tag{10}$$

Substitution of the expressions of $(\dot{u}_1^o)^2$ and $\left(\dot{u}_3^o\right)^2$ described above into Equation (7), the kinetic energy is then given as

$$T = \frac{1}{2}m_o\dot{w}_o^2 + \frac{1}{2}m_o\left[(A_1)^2 w_o^2\dot{w}_o^2 - 2A_1 w_o\dot{w}_o\dot{U}_B + \frac{8}{3}A_2 w_o^3\dot{w}_o\dot{U}_B + \left(\dot{U}_B\right)^2\right] \tag{11}$$

in which $A_1$ and $A_2$ are geometrical constants given as

$$A_1 = \int_0^L \left(\frac{\partial\phi}{\partial x}\right)^2 dx \tag{12}$$

and

$$A_2 = \int_0^L \left(\frac{\partial\phi}{\partial x}\right)^4 dx \tag{13}$$

and the first linear mode shape function $\phi(x)$ is given as

$$\phi(x) = 1 - \cos\left(\frac{\pi x}{2L}\right) \tag{14}$$

Once the final expression for the kinetic energy is known, the next step towards the derivation of equation of motion is obtaining the system's strain or potential energy which may be written as

$$U = \frac{1}{2}\iiint_V E\varepsilon_{xx}^2 dV = \frac{1}{2}\int_0^L\int_A E\varepsilon_{xx}^2 dA dx \tag{15}$$

In the system's strain field the component $\varepsilon_{xx}$ is composed by the contribution of the total contraction displacement $u_c$ and $u_r$. However, $u_c$ is very small when compared to $u_r$. Therefore, to simplify the analysis, the contribution of $u_c$ and of the gravitational field to the strain energy are ignored, thus giving

$$U = \frac{1}{2}\int_0^L \int_A E\left[z^2\left(w''\right)^2 - z^2\left(w''\right)^2\left(w'\right)^2\right] dAdx \tag{16}$$

By writing $w(x,t)$ as a function of $\phi(x)$ and $w_o(t)$ (Equation 8), the final expression for the strain energy truncated cubic terms in the system's equation of motion is given by

$$U = \frac{1}{2}EI_yB_1w_o^2 - \frac{3}{2}EI_yB_2w_o^4 + \ldots \tag{17}$$

where $I_y$ is the area moment of inertial about the y axis and, the geometrical constants $B_1$ and $B_2$ are given as

$$B_1 = \int_0^L \left(\phi''\right)^2 dx \tag{18}$$

$$B_2 = \int_0^L \left(\phi''\right)^2 \left(\phi'\right)^2 dx \tag{19}$$

The last step before deriving the system's equation of motion consists in obtaining the expression for the nonconservative forces acting on the system. Herein, it will be considered the action of three nonconservative forces. The first is the structural damping force which is modelled in terms of the generalized coordinates as $c_1\dot{w}_o$. The second is the aerodynamic drag damping force acting on the system (when in motion) and is proportional to the squared of the generalized velocity $c_2\dot{w}_o|\dot{w}_o|$. Both damping forces act in the negative direction of the virtual transversal displacement $\delta w_o$. The last nonconservative force is the acoustic excitation that is characterized as a single component sinusoidal force $F(t)$ applied at the center of gravity of the lumped mass and oriented along the $z$ direction. The external excitation $F(t)$ acts in the positive direction of the virtual transversal displacement $\delta w_o$. Physically $F(t)$ is originated from the dynamic pressure distribution over the structure $p(x,t)$, therefore $F(t)$ may be written as

$$F(t) = \int_A p(x,t)\,\phi(x)\,dx \tag{20}$$

Therefore, the nonconservative virtual work $\delta W_{nc}$ which is done on the system is given by

$$\delta W_{nc} = \left[-c_1\dot{w}_o - c_2\dot{w}_o|\dot{w}_o| + F(t)\right]\delta w_o \tag{21}$$

Since the nonconservative virtual work is defined as a function of the nonconservative generalized force $Q_{nc}$ as $\delta W_{nc} = Q_{nc}\delta w_o$, the generalized force $Q_{nc}$ is obtained as

$$Q_{nc} = \frac{\delta W_{nc}}{\delta w_o} = -c_1\dot{w}_o - c_2\dot{w}_o|\dot{w}_o| + F(t) \tag{22}$$

### 2.2 Equation of Motion

In the earlier section, the expressions for the kinetic energy $T$, strain energy $U$ and nonconservative generalized force $Q_{nc}$ were obtained. From these results, it possible to derive the system's equation of motion by using the well known Lagrange's equations (Meirovitch, 1970), which in turn, for the system under investigation is written as

$$\frac{d}{dt}\left(\frac{\partial T}{\partial \dot{w}_o}\right) - \frac{\partial T}{\partial w_o} + \frac{\partial U}{\partial w_o} = Q_{nc} \tag{23}$$

Computation of each term of the Lagrange's equation and substitution of the result the Equation (23) the following result is obtained

$$\left(1 + A_1^2w_o^2\right)\ddot{w}_o + \left(\frac{c_1}{m_o} + \frac{c_2}{m_o}|\dot{w}_o|\right)\dot{w}_o + \left(A_1^2\dot{w}_o^2 - A_1\ddot{U}_B + \frac{EI_yB_1}{mo}\right)w_o + \left(\frac{4}{3}A_2\ddot{U}_B - \frac{6EI_yB_2}{mo}\right)w_o^3 = \frac{F(t)}{mo} \tag{24}$$

Equation 24 represents an ordinary inhomogeneous nonlinear time-dependent differential equation. In addition, this equation holds both the axial contraction and the curvature nonlinear effects. If both the underlined and double underlined terms were ignored, this equation reduced to a classical linear damped forced model. On the other hand, if only the double underlined terms were ignored this equation reduces to the same obtained in (Gomes da Silva and Varoto, 2004) plus a forced term. Still, if the double underlined terms plus the nonlinear damping were ignored, this equation reduces to the same model obtained by in Cartmell (1990) plus a forced term.

Since the present work is focused on the dynamic response of a structure under the effects of combined acoustic external and parametric excitation it is considered that these excitations are can be written as

$$\ddot{U}_B(t) = -Q\lambda^2\cos(\lambda t + \varphi) = -Q_o\cos(\lambda t + \varphi) \tag{25}$$

and

$$F(t) = F_o \cos(\Omega t) \tag{26}$$

in which $Q_o$ and $F_o$ are the magnitudes of the base acceleration and external force, respectively, $\lambda$ and $\Omega$ are the parametric and external excitation frequencies and $\varphi$ is the phase shift between the excitations. Then, Equation (24) can be rewritten in the dimensionless final form by setting new dimensionless variables $w_o^* = A_1 w_o$ and $t^* = t/T_n$ in which $T_n$ is the period of free vibration. Hence, the system's final equation of motion is given by

$$\begin{aligned}\left(1+w_o^{*2}\right)\ddot{w}_o^* + H_1\dot{w}_o^* + H_2\dot{w}_o^*\left|\dot{w}_o^*\right| + \left[1+\dot{w}_o^{*2} + H_3\cos(\Theta t^* + \varphi)\right] w_o^* - \\ - \left[H_5 + H_4\cos(\Theta t^* + \varphi)\right] w_o^{*3} = H_6\cos(\Psi t^*)\end{aligned} \tag{27}$$

in which

$$H_1 = \frac{c_1 T_n}{m_o}; \qquad H_2 = \frac{c_2}{m_o A_1}; \qquad H_3 = Q_o A_1 T_n^2; \qquad H_4 = \frac{4A_2 Q_o T_n^2}{3A_1^2}; \qquad H_5 = \frac{6B_2 E I_y T_n^2}{m_o A_1^2}; \qquad H_6 = \frac{F_o A_1 T_n^2}{m_o}$$

$$\Theta = \lambda T_n; \qquad \Psi = \Omega T_n$$

## 3 Structure Modal Identification

In a previous paper (Gomes da Silva and Varoto, 2004) a detailed modal testing is performed on the structure under test by employing a transient excitation signal to obtain the structure's frequency response function in the vicinity of the first beam's bending natural frequency.

Figure 3 exhibits predicted FRFs for two different values for the lumped-mass $m_o$. The first value used comes from the lumped-mass plus the clamp bolts giving an equivalent mass of 63.6 g. The second value used $m_o = 118$ g comes from the best value of the lumped-mass in order to match with the experimental result, which can be claimed that for this value the theoretical and experimental curves matched very closely in the entire frequency range. On the other hand, the same behavior does not occur for the case where $m_o = 63.4$ g, even though this result also presents good agreement with the measured results. The theoretical result depicted on Figure 3 was obtained from basic theory and the system's modal parameters (Gomes da Silva and Varoto, 2004).

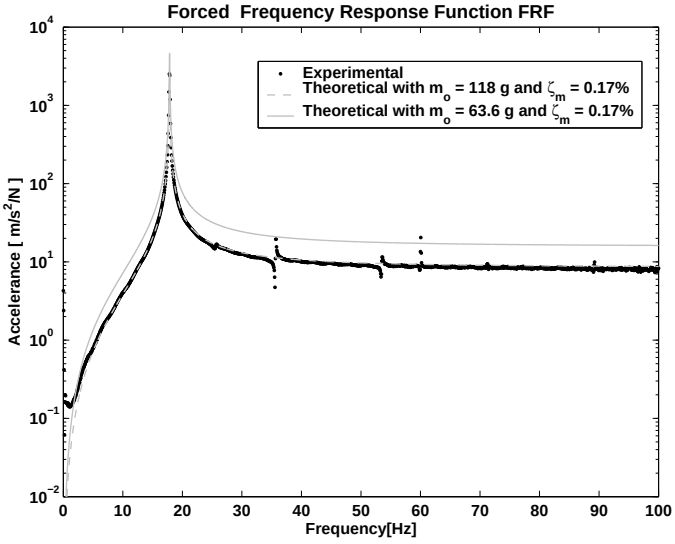


Figure 3: Comparative results for the accelerance FRF for the test structure.

### 3.1 The Acoustic Excitation Source

The acoustic excitation system used in the laboratory tests consists of a sealed 12" loudspeaker driven by a commercially available 500 $W$ power amplifier. Figure 4 corresponds to the sound pressure distribution over the structure for different input voltages. In this case, the loudspeaker is driven by a sinusoidal signal at 36 $Hz$ and the sound pressure is measured by a $1/2$" microphone in the vicinity of the beam. It can be claimed that for all three levels of inputs the shape of the sound pressure is nearly the same.

Since a pressure distribution is needed in Equation 20 the results shown in Figure 4 were curve fitted using a linear function and the following results were obtained and used with Equation 20

$$p_{170}(x) = 22.6x + 2.67 \tag{28}$$

$$p_{211}(x) = 27.4x + 3.37 \tag{29}$$

$$p_{255}(x) = 33.0x + 4.08 \tag{30}$$

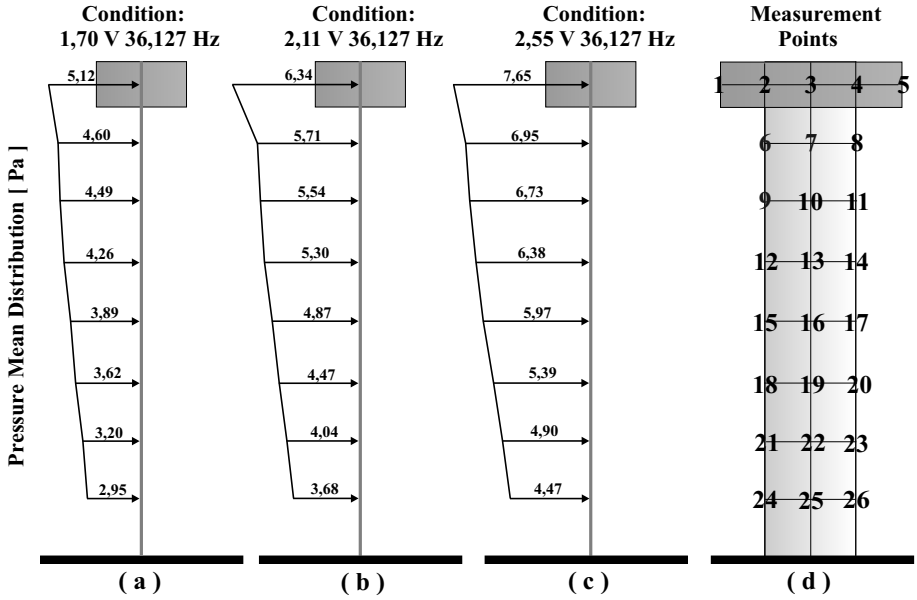


Figure 4: Experimental pressure distribution over the structure for acoustic source's input at 36.127 Hz and three different amplitudes: (a) 1.70 V; (b) 2.11 V; (c) 2.11 V and (d) measured points.

## 4 Nonlinear Tests

This section shows the results obtained from the nonlinear tests and a comparative analysis with numerically simulated results that were generated from the theoretical model in the previous sections. A total of three nonlinear tests were planed and conducted, as described below:

**NLT1** Exciting the structure using only the parametric excitation at $\lambda = 2\omega_n$ (principal parametric resonance case) for several amplitude levels $Q_o$.

**NLT2** Exciting the structure using both the external and parametric excitations, fixing $\lambda = \Omega = 2\omega_n$, and for several amplitude levels of the parametric excitation $Q_o$, and for three amplitude levels of the external excitation $F_o$, keeping the excitation signals in phase.

**NLT3** It is a test similar to the NLT2, however fixing the excitation signals out of phase.

In order to perform the nonlinear tests, the setup shown in Figure 5 was arranged.

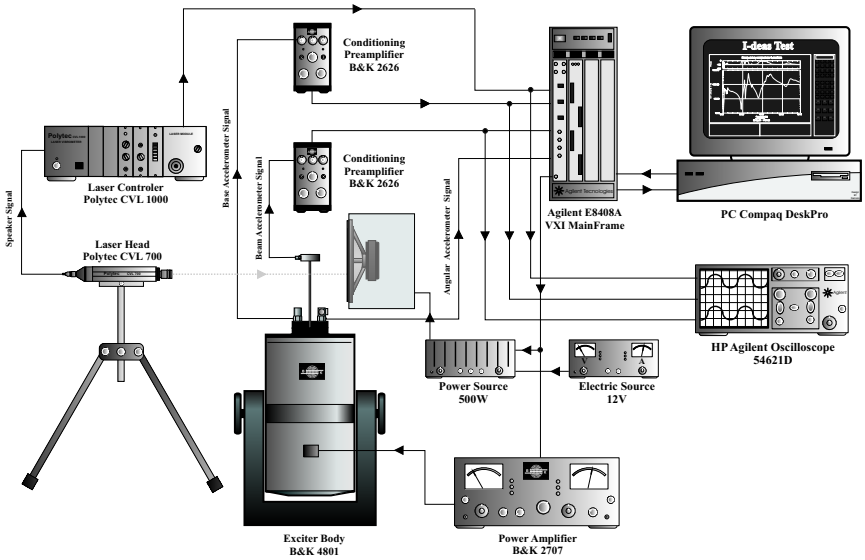


Figure 5: Experimental setup arranged to perform the nonlinear tests.

The structure under investigation was mounted on the steel base and this assemblage was fixed on the B&K 4801 vibration exciter table, which in turn is responsible by the parametric excitation. A linear single axis B&K 4371 (9.84 pC/g)

accelerometer was attached to the mounting base and is used to monitor the parametric excitation. The transversal external acoustic excitation is applied by the loudspeaker that is positioned parallel to the beam and mounted in a free-free condition. A Polytec CLV 1000 (50 mm/sV) laser vibrometer the external excitation by measuring the speaker cone velocity profile as it was done in the previous section. The excitation signals were generated by the Agilent E1432A board and sent to the power amplifiers before being applied to the test structure . A miniature accelerometer B&K 4370 (1.03 pC/g) was employed to capture the beam's response and a Kistler 8836M01 ($34\,\mu$V/rad/s$^2$) angular accelerometer is used to monitor possible rocking motions presented by shaker table. All input and output signals were gathered by the Agilent E1432 associated to the program MTS I-DEAS Test and a digital oscilloscope was used to monitor the phase shift between signals and to adjust the excitation levels.

Figure 6 shows the classical amplitude-response curve obtained from the experiments by following the strategy of test NLT1. This test was preformed by increasing the amplitude of parametric excitation from 0 to 44.5 m/s$^2$*RMS* while the frequency $\lambda$ was kept fixed at 36.132 Hz and then lowering the excitation amplitude at the same rate. A close look at this result reveals that between 25 and 30 m/s$^2$*RMS* the structure exhibits the principal parametric resonance phenomenon, and consequently a very high response amplitude is developed about 75 m/s$^2$*RMS*. In addition, this figure still shows that the structure responds differently depending on the sweeping direction of the excitation amplitude. The result shown in Figure 6 along with other experimental results obtained in the absence of the external acoustic excitation and not shown here were important to calibrate the analytical model previously obtained for the test structure and that will be used here along with the experimental results for comparison purposes.

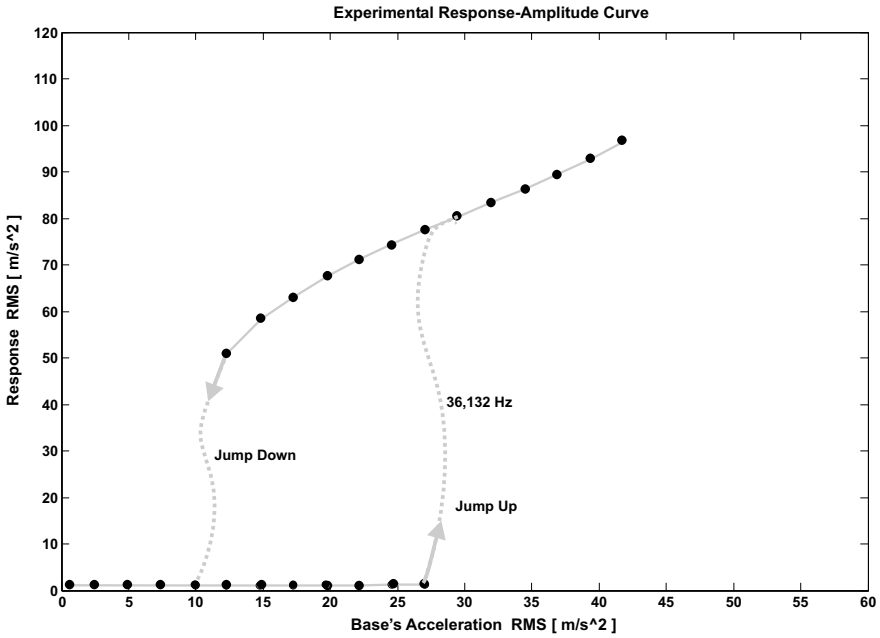


Figure 6: Experimentally determined response-amplitude curve without the presence of external excitation for principal parametric resonance case. Contemplate the first part of NLT1 nonlinear test.

The calibrated mathematical model will be compared with the measured data for two different situations, when the excitations (parametric and external) are in phase; and when the excitations are out of phase. In both cases, $\Omega = \lambda = 2\omega_n$. Figures 7 and 8 show the experimental and numerically simulated results corresponding to the situations where the excitation signals are maintained in phase (NLT2).A close examination in the detailed portion of the response reveals the interaction between the parametric and external excitation sources. With the development of the principal parametric resonance, the structure responds at its first bending natural frequency frequency $\omega_n = 18\ Hz$, plus harmonics in a increasing amplitude. Simultaneously, due to the presence of a external excitation the structure also responds, however at a frequency equal to external excitation $\Omega = 36\ Hz$ plus harmonics. When the ratio between the external response to parametric response is high there is a clear separation of these components, on the other hand, when this ratio is small, there is a merge of these response contributions and since the parametric resonance causes significantly higher vibration amplitudes, it prevails once the steady state regime is reached. A qualitative comparison between the experimental and numerically simulated results from Figures 7 and 8 shows a reasonably good agreement. Very similar numerical and experimental results were obtained when the excitation signals are out of phase (NLT3).

## 5 Concluding Remarks

In the present investigation, a detailed theoretical and experimental study was performed on a flexible structure under the combined action of two different excitations, an external from a acoustic source and a parametric from a electrodynamic shaker.

The obtained theoretical and experimental results shown many interested aspects on the dynamics of the tested structure. When the excitation frequency are commensurable, the structure does not reach a steady-state regime, except in a

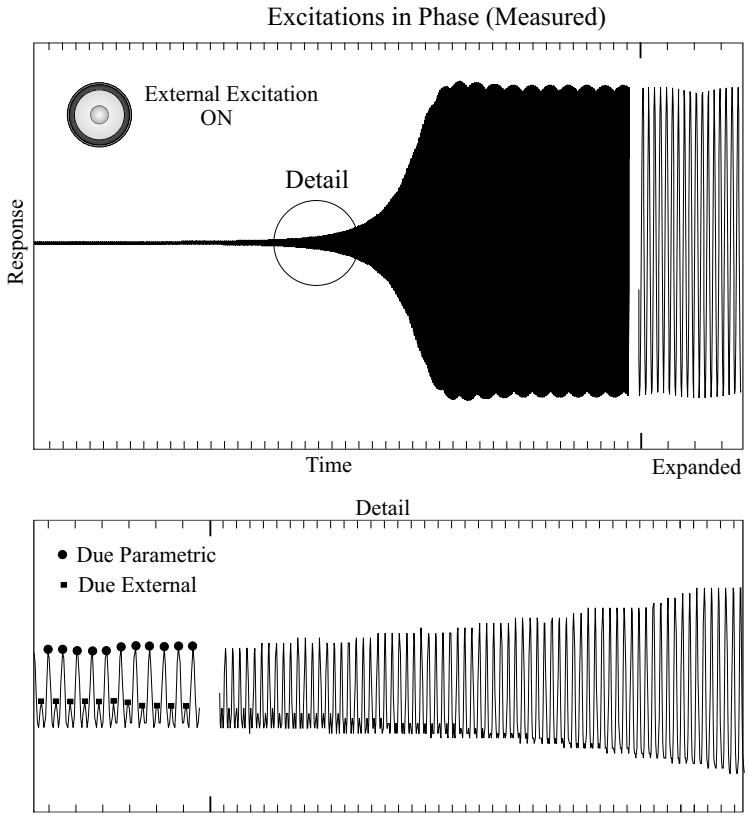


Figure 7: Predicted time-history, with the effects of combined parametric and external excitations, both in phase.

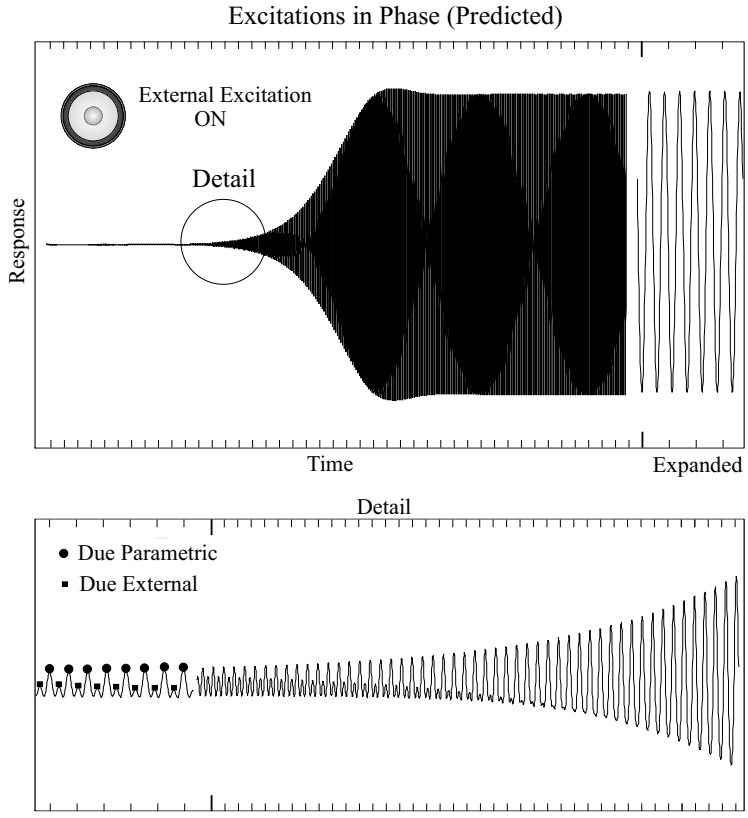


Figure 8: Predicted time-history, with the effects of combined parametric and external excitations, both in phase.

very special condition when $\Omega = \omega_n$ and $\lambda = 2\omega n$. Still in the commensurable case, it was shown that there is a general rule that determine the periodicity of the structure's response. On the other hand, in the incommensurate case it does not

obtained any rule that could be used to predict the periodicity of the response, even thought it was shown that exist a periodic motion for some special ratio between $\Omega$ and $\omega_n$ fixing $\lambda = 2\omega n$. In both cases, a fantastic and complex dynamic behavior was observed, showing the hard way to control they.

At the end, it also showed that all kind of exciting source have limitations and its own characteristics, which in turn, must to be known before they could be effectively used in experimental studies. For instance, if a certification does not had been made, probably some erroneous results using the acoustic source tuned about 18, Hz are present in the present investigation. Also due to the parametric certification, the effect of a small but present harmonic in the parametric excitation does not could be ignored and possible its effects will be attributed to the structure dynamic's behavior.

## 6 References


Anderson, T. J., Nayfeh, A. H., Balachandran, B., 1996, Experimental verification of the importance of the nonlinear curvature in the response of a cantilever beam, Journal of Vibration and Acoustics, V. 118, pp. 21-27.

Boresi, A. P., Schimidt, R. J., Sidebottom, O. M., 1993, Advanced Mechanics of Materials, Wiley.

Cartmell, M. P., 1990, "Introduction to linear, parametric and nonlinear vibration", Chapman and Hall, 1$^{st}$ edition.

Callinan, J. R., Galea, S. C., Sanderson, S., 1997, "Finite element analysis of bonded repairs to edge cracks in panels subjected to acoustic excitation", Composite Structures, V. 38 (1-4), pp. 649-660.

Gomes da Silva, D., Varoto, P. S., 2004, "On the sufficiency of classical response models in predicting the dynamic behavior of flexible structures", Proceedings of the 22nd IMAC, MI, USA.

Haquang, N., Mook, D. T., 1987a, A non-linear analysis of the interactions between parametric and external excitations, Journal of Sound and Vibration, V. 118, N. 3, pp. 425-439.

Haquang, N., Mook, D. T., 1987b, A non-linear structural vibration under combined parametric and external excitations, Journal of Sound and Vibration, V. 118, N. 2, pp. 291-306.

Meirovitch, L., 1970, Methods of Analytical Dynamics, McGraw-Hill.

Zavodney, L. D., Nayfeh, A. H., 1989, "The Non-linear response of a slender beam carrying a lumped mass to a principal parametric excitation:theory and experiment ", International Journal of Non-linear Mechanics, V. 24 N. 2, pp. 105-125.


## 7 Responsibility notice

The author is the only responsible for the printed material included in this paper.